Materials Letters 65 (2011) 1882–1884

Contents lists available at ScienceDirect

Materials Letters

journal homepage: www.elsevier.com/locate/matlet

Fe_3O_4 magnetic nanoparticles synthesis from tailings by ultrasonic chemical co-precipitation

Shen Wu [a], Aizhi Sun [a,*], Fuqiang Zhai [a], Jin Wang [a], Wenhuan Xu [a], Qian Zhang [a], Alex A. Volinsky [b]

[a] School of Material Science and Engineering, University of Science and Technology Beijing, Beijing 100083, China
[b] Department of Mechanical Engineering, University of South Florida, Tampa FL, 33620, USA

ARTICLE INFO

Article history:
Received 1 March 2011
Accepted 15 March 2011
Available online xxxx

Keywords:
Fe_3O_4 nanoparticles
Ultrasonic-assisted chemical co-precipitation
Surfaces
Magnetic properties
Nanomaterials

ABSTRACT

The aim of this study is to develop a new method for the preparation of high-value, environmentally friendly products from tailings. Magnetic Fe_3O_4 nano-powder was synthesized by ultrasonic-assisted chemical co-precipitation utilizing high purity iron separated from iron ore tailings by acidic leaching method. Magnetite particles with 15 nm average diameter were characterized by X-ray diffraction, field-emission scanning electron microscopy and vibrating sample magnetometer. Surfactant influence on particles shape and size was investigated. Fe_3O_4 nanoparticles coated with $C_{12}H_{25}OSO_3Na$ exhibit better dispersion and uniform size. The product consisted of ferrous ferrite (Fe3O4) nanosized cubic particles with a high level of crystallinity and exhibit super-paramagnetism based on magnetization curves lacking hysteresis.

1. Introduction

As developed mines are drying up, utilization of tailings is getting more attention [1]. Iron ore tailings are one of the most important industrial solid wastes. Due to their low iron content, exiguous granularity and complex composition, widely used extraction methods of magnetic separation or flotation are ineffective [2]. In this study high purity iron was separated from iron ore tailings by acidic leaching in order to alleviate the pressure of mining solid wastes on the environment. Magnetic Fe_3O_4 nanoparticles were synthesized with the purpose to explore sustainable economic way of recycling useful elements from mining solid wastes.

Iron ferrite, Fe_3O_4, is a traditional magnetic material used in magnetic storage media, solar energy transformation, electronics, ferrofluids and catalysis [3–7]. Several methods have been reported to synthesize Fe_3O_4 powders, including hydrothermal synthesis [8], microemulsion [9], chemical co-precipitation [10], oxidation of $Fe(OH)_2$ by H_2O_2 [11], R-ray irradiation [12], microwave irradiation [13], etc. Co-precipitation is the simplest and cheapest synthesis method. However, this method does not yield uniform nano-scale Fe_3O_4 particles directly without further separation. Therefore, uniform Fe_3O_4 nanoparticles preparation method with excellent dispersion is needed.

In this paper high purity iron was separated from tailings, and then magnetic Fe_3O_4 nanoparticles were synthesized by ultrasonic-assisted chemical co-precipitation. Utilizing iron particles coated with surface active agent, instead of vacuum or protective gas processes, the problems of Fe^{2+} oxidation and particles agglomeration were successfully solved.

2. Experimental details

2.1. Separation of iron

Iron ore tailings were weighed (100 g), and mixed with 37.5 wt.% hydrochloric acid (HCl). Then pickling was filtered out and collected. An appropriate amount of hydrogen peroxide (H_2O_2) was added to the filtrate so that all iron could exist in the Fe^{3+} form. Filtrate was heated to 60 °C, and its pH value was adjusted to 3.2 by adding an appropriate amount of concentrated ammonia. As a result, Fe was separated from tailings and precipitated into $Fe(OH)_3$. Finally, some amount of $Fe(OH)_3$ was washed repeatedly with de-ionized water, and then calcined into Fe_2O_3. Iron elemental percentage was calculated and analyzed, providing basis for the following Fe_3O_4 nanoparticles synthesis.

2.2. Fe_3O_4 nanoparticles preparation

Fe_3O_4 nanoparticles co-precipitation preparation flow chart is shown in Fig. 1. $Fe(OH)_3$ precipitate was washed several times with de-ionized water. Then $FeCl_3$ solution was obtained by $Fe(OH)_3$ precipitate dissolution with hydrochloric acid. By adding measured amount of $FeSO_4 \cdot 7H_2O$, Fe^{3+} and Fe^{2+} molar ratio in $FeCl_3$ solution was adjusted to 1.5:1. Under ultrasonic agitation, black precipitate was produced immediately by adding sodium hydroxide (NaOH). The principle reaction is:

$$Fe^{2+} + 2Fe^{3+} + 8OH^- \rightarrow Fe_3O_4 + 4H_2O. \qquad (1)$$

---

[*] Corresponding author. Tel.: +86 10 82376835; fax: +86 10 62333375.
E-mail address: sunaizhi@126.com (A. Sun).

0167-577X/$ – see front matter © 2011 Elsevier B.V. All rights reserved.
doi:10.1016/j.matlet.2011.03.065

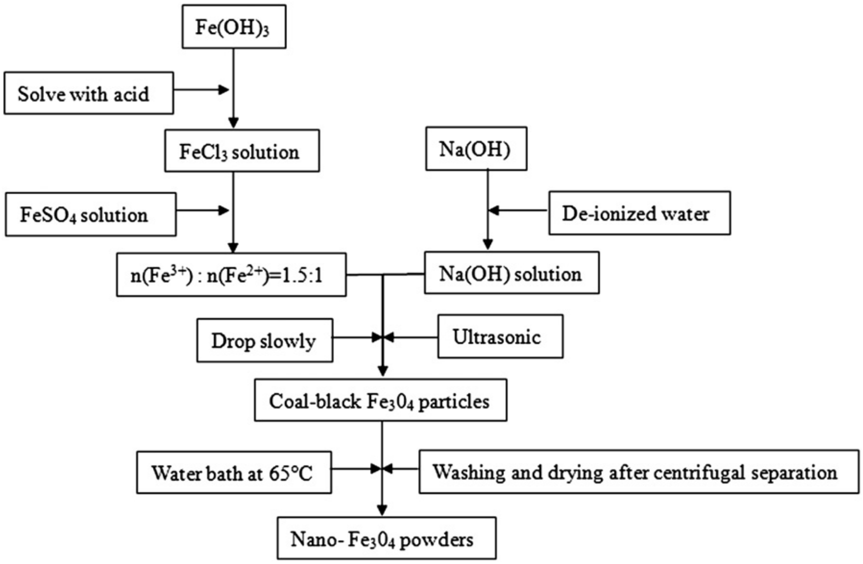

Fig. 1. Processing steps for Fe_3O_4 nanoparticles preparation.

Obtained Fe_3O_4 precipitate was aged at 65 °C for 30 min in ultrasonic water bath. To purify prepared Fe_3O_4 particles, the samples were washed repeatedly with de-ionized water and ethanol until pH level of 7 was reached. Particles were then dried at 74 °C in vacuum.

X-ray powder diffraction (XRD) patterns were recorded using Philips APD-10 X-ray diffractometer with Cu Kα radiation. The morphology and size of particles were observed in field-emission scanning electron microscope (FE-SEM, ZEISS ULTRA 55, Germany). Saturation magnetization was measured with vibrating sample magnetometer (VSM) (LDJ 9600, LDJ Electronics, USA) at 300 K in ±20 kOe applied field.

3. Results and discussion

3.1. Fe_3O_4 nanoparticles crystal structure and morphology

Fig. 2 shows X-ray diffraction patterns of synthesized Fe_3O_4 nanoparticles.

Comparing XRD pattern of synthesized particles with the standard diffraction spectrum (JCPDS: 65–3107), the synthesized product is crystalline Fe_3O_4. The sharpness of XRD reflections clearly shows that the synthesized Fe_3O_4 is highly crystalline. The average particle size was calculated to be 19.4 nm using the Sherrer's equation [14]:

$$L = K\lambda / \beta \cos\theta \tag{2}$$

where L is equivalent of particles average core diameter; K is the grain shape factor (K = 0.94); λ is the incident X-ray wavelength; β denotes the full width at half-maximum (in radians) of the highest intensity 311 powder diffraction reflection, and θ is the corresponding diffraction angle ($2\theta = 35.5748°$).

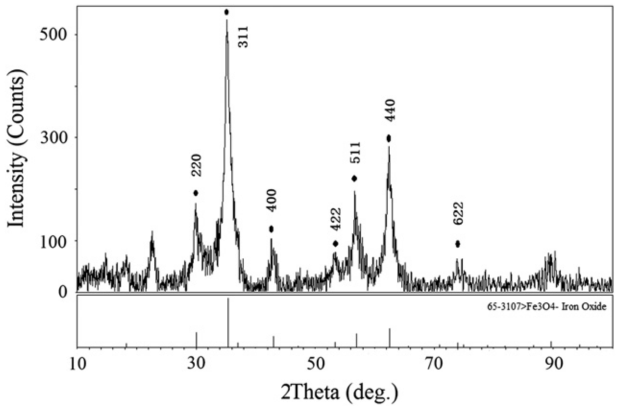

Fig. 2. XRD pattern of obtained samples.

Fig. 2 displays diffraction reflections broadening caused by grains refinement of Fe_3O_4 nanoparticles. A large number of generated surface defects with high specific surface area and particles distortions caused by high interfacial tension of smaller grains contribute to diffraction reflection broadening. In addition, particles could not be completely dispersed only by ultrasonic dispersion. Nanoparticles can be crystalline, amorphous or quasi-crystalline [15], therefore XRD particle size calculations are not quite accurate, justifying FE-SEM observations.

Elemental analysis of calcined product is shown in Table 1. In a pure Fe_2O_3 compound iron content is 70%, thus the product purity can be calculated using Eq. (3):

$$\text{Purity} = (68.88 / 70) \times 100\% = 98.4\%. \tag{3}$$

This result indicates that impurities exist corresponding to additional reflections in Fig. 2.

Fe_3O_4 nanoparticles were dispersed by ultrasound in alcohol after repeated washing. Corresponding FE-SEM micrograph is shown in Fig. 3(a), where particles are homogeneously dispersed. Particles are almost spherical with 15 nm average diameter.

3.2. Surfactant effects on preparation

In order to investigate the effect of surfactant on magnetite particles preparation, adding measured amount of $C_{12}H_{25}OSO_3Na$, Fe^{3+} and $C_{12}H_{25}OSO_3Na$ molar ratio in the reaction solution was adjusted to 12:1.

Table 1
EDS analysis after calcination.

Element	Element %	Atomic %
O K	27.81	56.43
Al K	1.61	1.94
Si K	0.62	0.72
Ca K	1.08	0.88
Fe K	68.88	40.04
Total	100.00	100.00

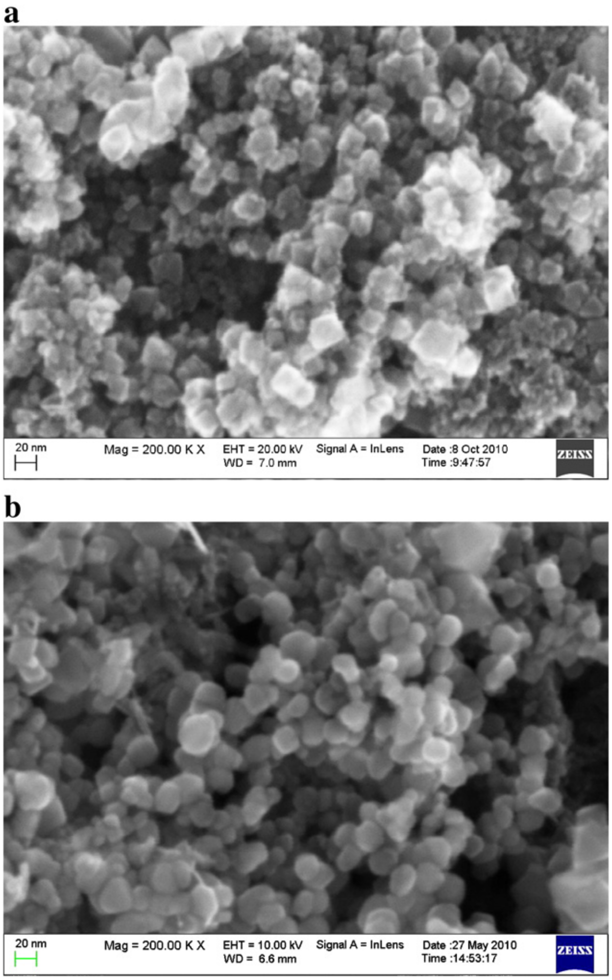

Fig. 3. FE-SEM image of Fe_3O_4 nanoparticles: (a) without $C_{12}H_{25}OSO_3Na$ and (b) with added $C_{12}H_{25}OSO_3Na$.

Corresponding field emission electron microscope micrographs are shown in Fig. 3, where Fe_3O_4 nanoparticles coated with $C_{12}H_{25}OSO_3Na$ exhibit better dispersion and uniform size. When $C_{12}H_{25}OSO_3Na$ dissolves in water, its hydrophilic oxygen atoms are located in the outer branches of the molecular chain, while hydrophobic alkyl (—CH_2—) radical forms the inner chain. Therefore, S—O bond's oxygen atoms could bond with highly active Fe_3O_4 by coordinate bond, which shows that $C_{12}H_{25}OSO_3Na$ possess chemical adsorption ability.

3.3. Magnetic properties

Magnetic properties of Fe_3O_4 nanoparticles were measured by VSM at 300 K, shown in Fig. 4. No magnetic hysteresis loop appears in magnetization curve of Fe_3O_4 nanoparticles, exhibiting super-paramagnetism with 74.86 emu/g saturation magnetization.

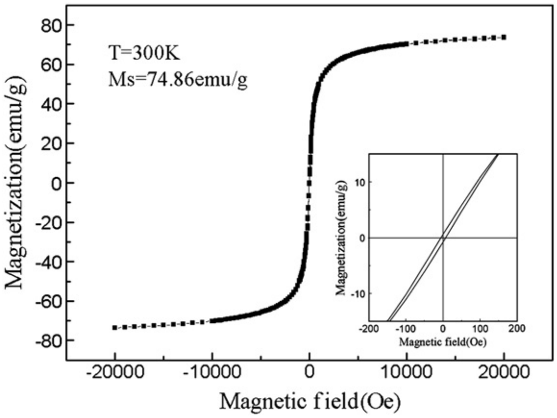

Fig. 4. Magnetic curve of synthesized particles at 300 K.

4. Conclusions

Utilizing high purity iron separated from iron ore tailings by acidic leaching method, nano-scale magnetic Fe_3O_4 powder was synthesized by ultrasonic-assisted chemical co-precipitation. As a result, Fe_3O_4 particles with 15 nm diameter exhibited super-paramagnetic behavior, and $C_{12}H_{25}OSO_3Na$ was added as surface active agent, assisting to obtain Fe_3O_4 nanoparticles with homogenous size and shape distribution. In the present study nanoparticles synthesis requires no protecting gas, and can be easily implemented because it is simple and environmentally friendly.

References

[1] Watson JHP, Beharrell PA. Miner Eng 2006;19:1580–7.
[2] Chen LZ, Ren NQ, Xiong DH. Met Mine 2006;10:75–7.
[3] Yamguchi K, Matsumoto K, Fiji T. J Appl Phys 1990;67:4493–5.
[4] Odenbach S. Adv Colloid Interface Sci 1993;46:263–82.
[5] Atarshi T, Imai T. J Magn Magn Mater 1990;85:3–6.
[6] Caceres PG, Behbehani MH. Appl Catal A 1994;109:211–23.
[7] Chikov V, Kuznetsow A. J Magn Magn Mater 1993;122:367–70.
[8] Fan R, Chen XH, Gui Z. Mater Res Bull 2001;36:497–502.
[9] Zhang DE, Tong ZW, Li SZ, Zhang XB, Ying AL. Mater Lett 2008;62:4053–5.
[10] Jiang WQ, Yang HC, Yang SY, Horng HE, Hung JC, Chen YC, et al. J Magn Magn Mater 2004;283:210–4.
[11] Yu LQ, Zheng LJ, Yang JX. Mater Chem Phys 2000;66:6–9.
[12] Wang SZ, Xin HW, Qian YT. Mater Lett 1997;33:113–6.
[13] Khollam YB, Dhage SR, Potdar SB. Mater Lett 2002;56:571–7.
[14] Warren E. X-ray diffraction: Dover, Canada; 1990.
[15] Bang Y. Nanometer era: reality and dream, Beijing; 2001.